JACS
JOURNAL OF THE AMERICAN CHEMICAL SOCIETY

pubs.acs.org/JACS

Article

Energetically More Stable Singlet Cyclopentane-1,3-diyl Diradical with π-Single Bonding Character than the Corresponding σ-Single Bonded Compound

Qian Liu,[†] Keita Onishi,[†] Yuki Miyazawa, Zhe Wang, Sayaka Hatano, and Manabu Abe*

Cite This: *J. Am. Chem. Soc.* 2023, 145, 27089−27094

Read Online

ACCESS | Metrics & More | Article Recommendations | Supporting Information

ABSTRACT: Carbon−carbon σ-single bonds are crucial for constructing molecules like ethane derivatives ($R_3C{-}CR_3$), which are composed of tetrahedral four-coordinate carbons. Molecular functions, such as light absorption or emission, originate from the π-bonds existing in ethylene derivatives ($R_2C{=}CR_2$). In this study, a relatively stable cyclopentane-1,3-diyl species with π-single bonding system (C−π−C) with planar four-coordinate carbons is constructed. This diradicaloid is energetically more stable than the corresponding σ-single bonding system. The π-electron single bonding system provides deeper insights into the chemical bonding and the physical properties derived from the small energy gaps between the bonding and antibonding molecular orbitals.

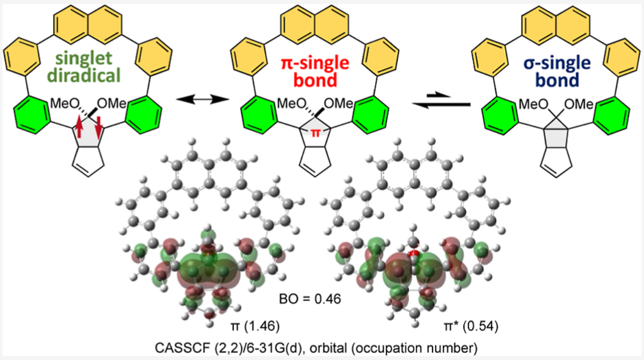

INTRODUCTION

Carbon atoms can be connected through two types of bonds: σ- and π-bonds (Figure 1a). The σ-bond, as observed in ethane derivatives ($R_3C{-}CR_3$), has a high bonding energy (368 kJ mol^{-1} for $H_3C{-}CH_3$)[1] and is crucial in constructing molecules. π-Electron systems, such as ethylene derivatives $R_2C{=}CR_2$ (π-bond energy in $H_2C{=}CH_2$: 272 kJ mol^{-1}),[2] are significant because they impart molecular functions such as light absorption and emission and facilitate electron transfer and chemical reactions. Therefore, the development of new π-conjugated molecules, such as those capable of harvesting solar energy, is a highly coveted research area.[3−5]

As σ-bonds are strong, C−C σ-single bonding that exists in the ethane molecule is possible. However, π-bonding between two carbon atoms is believed to occur only through strong σ-bonds, which primarily connect carbons. Examples of such bonding are ethylene derivatives. In 2000, during the research on cyclopentane-1,3-diradicals (DR-**1**),[6] which are crucial intermediates in the C−C bond homolysis[7,8] of σ-**1**, we realized that a π-single bonding structure (π-**1**) was theoretically possible in the singlet state (S-DR-**1**).[9] This structure comprises two planar four-coordinate carbons[10−12] linked only by a π-bond (C−π−C), without any σ-bond (Figure 1b). The highest occupied molecular orbital (HOMO)−lowest unoccupied molecular orbital (LUMO) energy gap of C−π−C bonds is expected to be much smaller than those of C−C σ-bonds (C−C distance $d \approx 155$ pm) and C=C σ,π-bonds ($d \approx 135$ pm), and this can be attributed to the long distance ($d \approx 220$ pm) between the carbons; i.e., the energy decreases in the order $\Delta E^{\sigma}_{\mathrm{HL}} > \Delta E^{\sigma\pi}_{\mathrm{HL}} > \Delta E^{\pi}_{\mathrm{HL}}$. Consequently, the π → π* absorption band appears in the visible to near-infrared region (Figure 1a). Compound π-**2** was prepared to experimentally verify these results (Figure 1c); this compound exhibited a strong absorption band at 500−700 nm, with $\lambda_{\max}$ at ∼ 580 nm ($\varepsilon \approx 5000\ \mathrm{M}^{-1}\ \mathrm{cm}^{-1}$).[13,14] Quantum chemical calculations accurately reproduced the electronic excitation energy from the HOMO (π-bonding orbital) to LUMO (π-antibonding orbital) in the π-electron system, demonstrating that π-**2** is not a perfect closed-shell singlet molecule that exhibits the character of an open-shell singlet diradical depicted in S-DR-**2**.[15] Hereon, the diradical resonance structure is omitted to simplify the explanation of the π-single bonding character. Because the σ-bond is stronger than the π bond, π-**2** was short-lived with a lifetime of ∼ 300 ns at 293 K in benzene, yielding quantitatively more energetically stable σ-bonded σ-**2**. Compound σ-**2** was computed to be energetically more stable than π-**2** by 63.7 kJ mol^{-1}. In contrast to short-lived carbon-centered radical species, several heteroatom-centered π-single bonds in four-membered heterocycles have been isolated since 2002, benefiting from the unique characteristics of heteroatoms (Figure 1d).[16−21] In this study,

Received: October 5, 2023
Revised: November 2, 2023
Accepted: November 3, 2023
Published: November 15, 2023

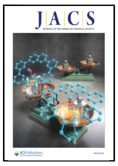

ACS Publications

https://doi.org/10.1021/jacs.3c10971

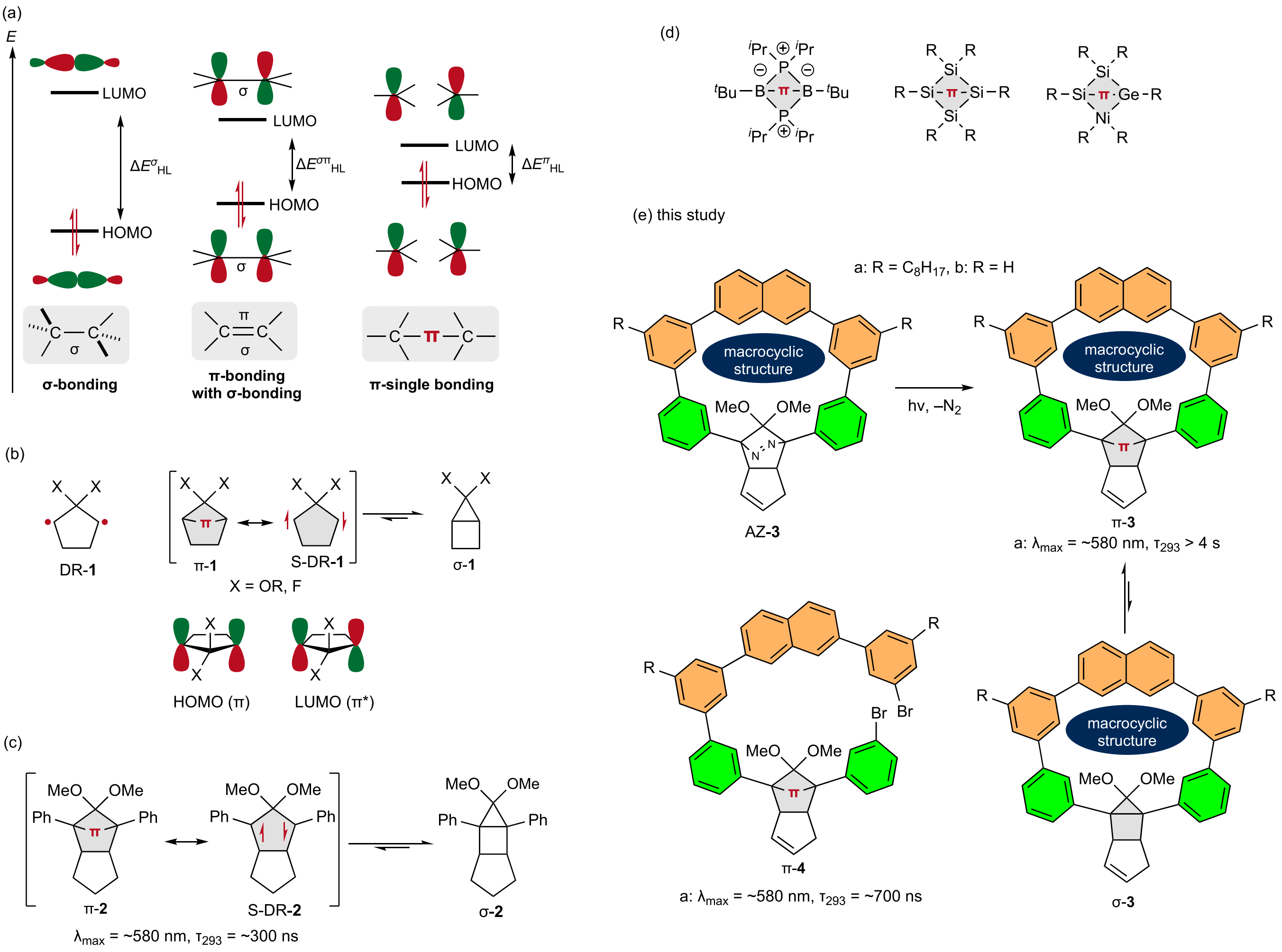

Figure 1. (a) HOMO−LUMO gaps; (b) *π*-single bonding in cyclopentane-1,3-diyl diradicals; (c) detectable *π*-single bonding; (d) isolated *π*-single bonded compounds in heterocyclic structures; (e) this study: long-lived *π*-single bonding.

we reveal that *π*-**3**, embedded in a macrocyclic structure, was energetically more stable than the corresponding *σ*-bonding compound (*σ*-**3**). Compound *π*-**3** exhibits a long lifetime of more than 4 s at 293 K (Figure 1e). The macrocyclic structure was designed to significantly increase the molecular strain of *σ*-**3** to alter the energy relationship between the *σ*- and *π*-bonds.[22]

RESULTS AND DISCUSSION

Azoalkane AZ-**3a** (R=C_8H_{17}), a precursor of *π*-**3a**, was synthesized in 12 steps (Scheme S1). The structural assignment of AZ-**3a** was established through ^{1}H-nuclear magnetic resonance (NMR) spectroscopy, ^{13}C NMR spectroscopy, mass spectrometry (MS), and single-crystal X-ray structural analysis (Figure S1). Compound *π*-**3a** was generated through the photochemical denitrogenation of AZ-**3a** (0.5 mM) in benzene under vacuum conditions and analyzed through transient absorption (TA) spectroscopy via the laser flash photolysis (LFP) technique conducted using a Nd/YAG laser (λ_{exc} = 355 nm, 4.5 mJ/pulse, 5 ns pulse width; Figures 2 and S2). The strong absorption band at ∼ 580 nm, assigned to *π*-**3a**, was observed after LFP (Figure 2a). The lifetime ($\tau = 1/k_d$) of *π*-**3a** was determined to be 262 ms at 293 K (Figure 2b), which is significantly longer than those of *π*-**2** and *π*-**4a** (lacking a macrocyclic ring; ∼ 300 and ∼ 700 ns at 293 K, respectively (Figure S3). The triplet state was not detected by EPR (Figure S4). Temperature dependence on *τ* was examined in a toluene solution under vacuum conditions (Figure S5) to obtain the activation parameters of the fall process. Surprisingly, the effect of the temperature on *τ* was negligible. The *τ* values were 250 ms at 304 K, 273 ms at 292 K, 320 ms at 279 K, 340 ms at 267 K, and 365 ms at 254 K. Using these values, activation parameters E_a, $\log(A/s^{-1})$, $\Delta H^{\ddagger}$, $\Delta S^{\ddagger}$, and $\Delta G^{\ddagger}_{298}$ were determined to be 5.0 kJ mol^{-1}, 1.45, 2.7 kJ mol^{-1}, −224.9 J mol^{-1} K^{-1}, and 69.7 kJ mol^{-1}, respectively. This negligible temperature effect indicates that the rate-determining step does not involve thermally activated bond-making or bond-breaking processes.

We noticed that the lifetime of *π*-**3a** was significantly dependent on the intensity of the monitor light in the LFP experiments (Figure 2b). The *τ* values were 0.17 s at 37 mW, 0.41 s at 12 mW, and 1.5 s at 6 mW at 293 K. In addition, photochemical bleaching of the 580 nm species was observed when the second laser flash (λ_{exc} = 580 nm from the optical parametric oscillator laser) was introduced 500 ms after the first laser flash at λ_{exc} = 355 nm (Figure S6). To appropriately obtain the thermal decay process of *π*-**3a**, we modified the LFP setup by removing the focal lens, which effectively reduced the monitor light intensity and prevented the diffusion effects that could shorten the lifetime. The lifetime of *π*-**3a** was found to

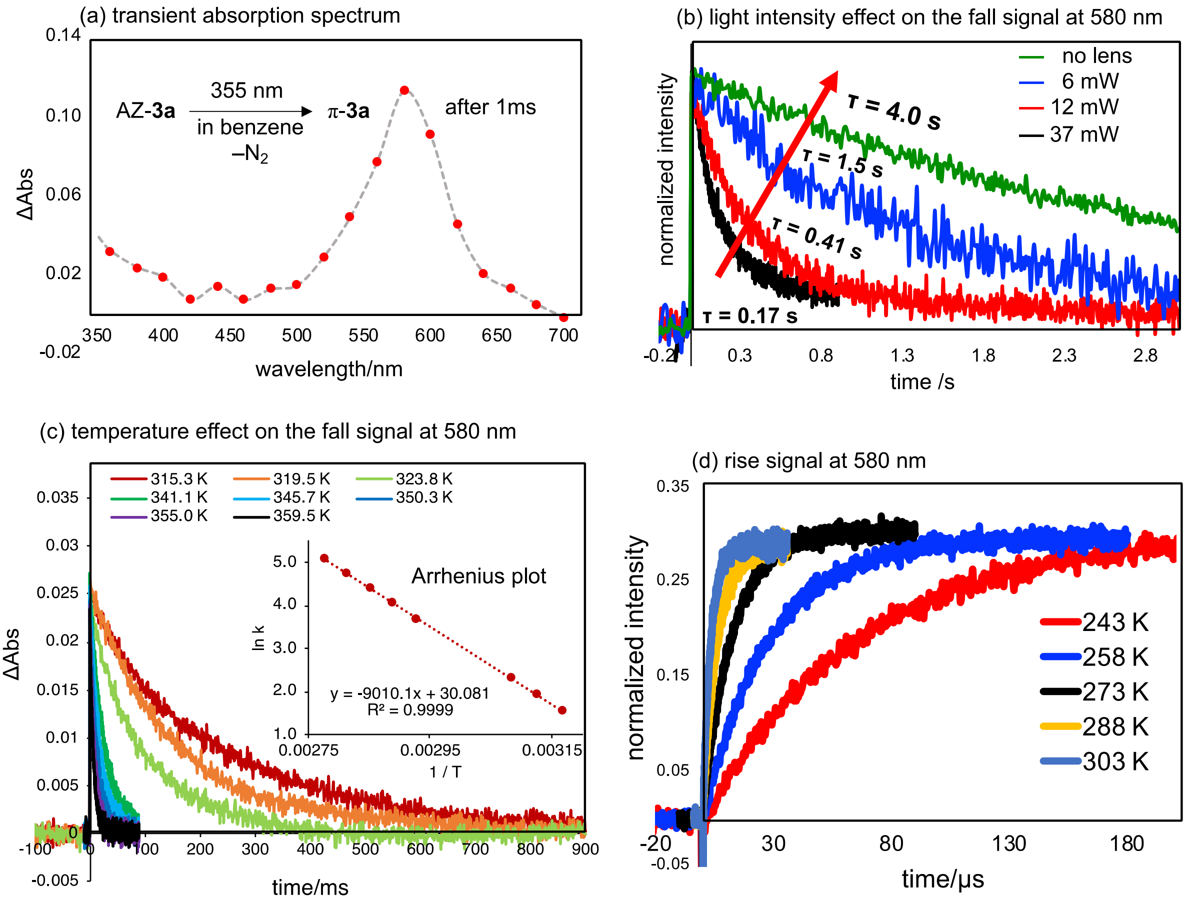

Figure 2. Transient absorption spectroscopy via LFP (355 nm) of AZ-**3a** (0.5 mM). (a) Transient absorption spectrum in benzene after 1 ms at 293 K; (b) effect of monitor light intensity on the lifetime of *π*-**3a** in toluene at 293 K; (c) temperature dependence of the lifetime of *π*-**3a** in toluene; and (d) generation of *π*-**3a** in the photolysis of AZ-**3a** in toluene.

Scheme 1. Photochemical Denitrogenation Reaction of AZ3[a]

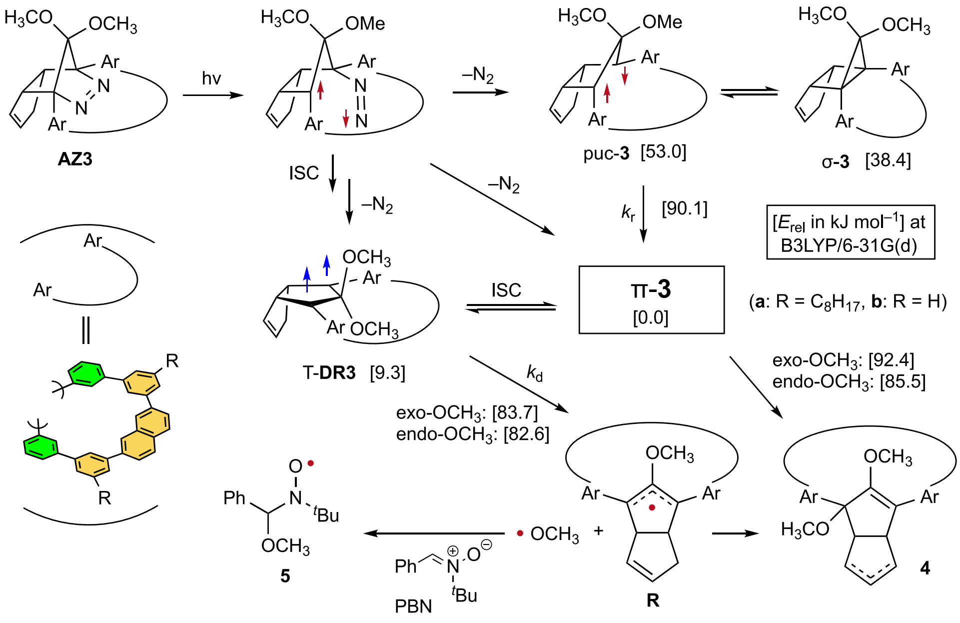

[a] The values in parentheses are relative electronic energy (E_{rel}) after zero point energy corrections calculated at the (R,U)B3LYP/6-31G(d) level of theory for **b** (R=H).

---

be 4.0 s at 293 K (at 6 mW of monitor light with no focal lens; green signal in Figure 2b). The temperature dependence of the lifetime ($\tau = 1/k_d$) of *π*-**3a** in an argon-saturated toluene solution was reinvestigated in the temperature range of 315−

https://doi.org/10.1021/jacs.3c10971
J. Am. Chem. Soc. 2023, 145, 27089−27094

360 K to minimize the photochemical decomposition of *π*-**3a** (Figure 2c). From these experiments, we determined the activation parameters E_a, log(A/s^{-1}), $\Delta H^{\ddagger}$, $\Delta S^{\ddagger}$, and $\Delta G^{\ddagger}_{298}$ of the decay (k_d) of *π*-**3a** to be 74.9 kJ mol^{-1}, 13.1, 72.1 kJ mol^{-1}, −4.1 J mol^{-1} K^{-1}, and 73.4 kJ mol^{-1}, respectively, from the Arrhenius (Figure 2c) and Eyring plots (Figure S7). Using the obtained activation parameters, the lifetime of *π*-**3a** at 293 K was extrapolated to be 1.9 s, which is slightly shorter than the experimentally obtained value of 4.0 s. This indicated the occurrence of slight photochemical decomposition during the temperature dependence experiments at 30 mW of monitor light.

During the TA analysis via LFP of AZ-**3a**, surprisingly, the rising process of *π*-**3a** (λ_{max} = 580 nm) was observed at the *μ*s time scale (Figure 2d). For example, the rising rate constant (k_r) at 288 K for benzene was found to be $k_r = 1.28 \times 10^5$ s^{-1} ($1/k_r$ = 7.8 *μ*s). The previously reported photochemical denitrogenation of $CH_3{-}N{=}N{-}CH_3$ involves a stepwise denitrogenation process, $CH_3{-}N{=}N{-}CH_3 \rightarrow CH_3{-}N{=}N\cdot + \cdot CH_3 \rightarrow 2CH_3\cdot + N_2$, at the fs time scale.[23] Therefore, the rising process observed at 580 nm during LFP of AZ-**3a** did not correspond to a denitrogenation process (Scheme 1). The temperature dependence of k_r was investigated in toluene solution under vacuum conditions to gain further insights into the rising process at 580 nm (Figures 2d and S8). Interestingly, the rate constants were found to be significantly dependent on the temperature, and activation parameters E_a, log(A/s^{-1}), $\Delta H^{\ddagger}$, $\Delta S^{\ddagger}$, and $\Delta G^{\ddagger}_{298}$ were determined to be 38.4 kJ mol^{-1}, 12.1, 36.1 kJ mol^{-1}, −21.2 J mol^{-1} K^{-1}, and 42.4 kJ mol^{-1}, respectively. The large pre-exponential value, log(A/s^{-1}), clearly indicates that the rising process of *π*-**3a** at 580 nm is not the spin-forbidden intersystem crossing process from T-**DR3a** to *π*-**3a**, but rather a chemical transformation.

In our previous study, we successfully elucidated the reactivity of *π*-**2**, verifying that this compound was thermally equilibrated with the corresponding puckered diradical puc-**2** and the most stable ring-closing compound *σ*-**2**.[14] Therefore, the LFP results for AZ-**3a** can be rationalized using the mechanism shown in Scheme 1. Consequently, the rising process of *π*-**3a** observed during the TA analysis was attributed to the transformation from *σ*-**3a** to *π*-**3a** via puc-**3a**, suggesting that *σ*-**3a** was energetically less stable than *π*-**3a**. This conclusion was further supported by the fact that no *σ*-**3a** was detected; however, relatively complex products were obtained in the photochemical denitrogenation of AZ-**3a**. NMR and MS analyses revealed these products to be a regio- and stereochemical mixture of methoxy-migrated vinyl ethers **4** ([M + Na]$^+$ = 818.50842 (Figure S9), Scheme 1), suggesting the generation of the methoxy radical $CH_3O\cdot$. Furthermore, we conducted photochemical denitrogenation of AZ-**3a** in the presence of a radical trapping agent, *N*-*tert*-butyl-*α*-phenylnitrone (PBN), to verify the generation of $CH_3O\cdot$. 1,1-Dimethylethyl methoxyphenylmethyl nitroxide (**5**), a known compound, was detected through electron paramagnetic response with hyperfine coupling constants of a_N = 13.6 G and $a_{H\beta}$ = 2.0 G (Figure S10).[24,25]

As mentioned above, time-resolved TA analysis revealed the unprecedented rise and fall dynamics of relatively stable *π*-**3a**. Quantum chemical calculations were conducted for the structural optimization of *π*-**3b** (R=H), T-**DR3b**, *σ*-**3b**, and puc-**3b** at the (R,U)B3LYP/6-31G(d) level of theory[26,27] to obtain deeper insights into this unprecedented phenomenon and unique bonding system (Scheme 1 and Figure S11). The complete active space self-consistent field (CASSCF) method[28] was utilized to evaluate the electronic configuration of *π*-**3b** (Figure 3).

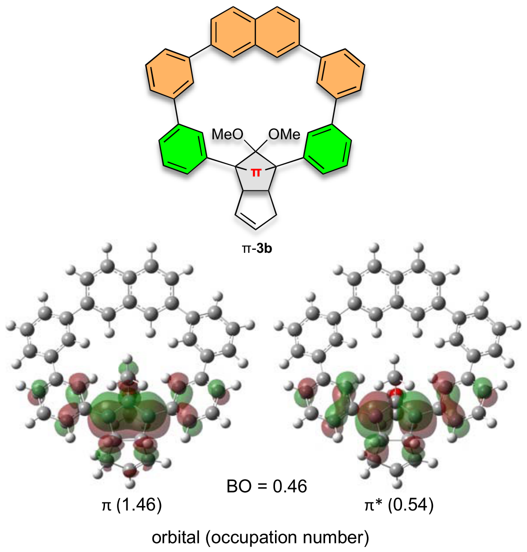

Figure 3. Visualized bonding orbital (*π*) and antibonding orbital (*π**) and their electron occupation numbers in *π*-**3b** computed at the CASSCF(2/2)/6-31G(d) level of theory.

Consistent with the experimental findings for *π*-**3a**, the singlet state of *π*-**3b** was energetically more stable than its triplet state T-**DR3b** and *σ*-**3b** by 9.3 and 38.4 kJ mol^{-1}, respectively. As mentioned in the Introduction section, *σ*-**2** was computed to be energetically more stable than *π*-**2** by 63.7 kJ mol^{-1} at the same level of theory. This switch in the energy relationship between the *σ*- and *π*-bonded compounds was rationalized by the strain energy (SE) induced by the macrocyclic structure[29−33] of *σ*-**3b**. The SE of *σ*-bonded *σ*-**3b** was computed to be 75.6 kJ mol^{-1} higher than that of *π*-**3b** (Table S2). The energetic stability of *π*-**3b** supports the idea that the rising process of *π*-**3a** is induced by the less energetically stable *σ*-**3a** via puc-**3a** (Scheme 1). The transition state for the transformation from puc-**3b** to *π*-**3b** was computed at the same theoretical level to confirm the reaction pathway from puc-**3** to *π*-**3** (Scheme 1). A transition-state structure with one imaginary frequency was observed in which one of the two methoxy (OCH_3) groups passed through the macrocyclic structure (Figure S11 and Movie S1). The total electronic energy of the transition state, including the zero-point vibrational energy, was 37.1 kJ mol^{-1} higher than that of puc-**3b** in the gas phase (Scheme 1), which was 90.1 kJ mol^{-1} higher than that of *π*-**3b**. The computed activation parameters $\Delta H^{\ddagger}$ and $\Delta G^{\ddagger}_{298}$ at 298.150 K and 1.0 atm were found to be 34.7 and 42.6 kJ mol^{-1}, respectively. The computed values are very consistent with the experimentally obtained activation values (Figure 1d).

The potential energy surfaces of the bond breaking between the acetal carbon and CH_3O oxygen were computed in both the singlet and triplet states, *π*-**3b** and T-**DR3b**, respectively (Scheme 1 and Figure S12), to comprehend the decay process of *π*-**3a** (Figure 1c). Interestingly, the concerted 1,2-migrations of the CH_3O group with an activation energy of 92.4 kJ mol^{-1} for the exo isomer and 85.5 kJ mol^{-1} for the endo isomer directly produced **4** via the reaction from *π*-**3b**. The lower activation energies for bond breaking in T-**DR3b** (74.4 kJ mol^{-1} for exo-CH_3O and 73.3 kJ mol^{-1} for endo-CH_3O) led to the generation of a pair of radicals, namely, the methoxy radical ($CH_3O\cdot$) and the allylic radical. Indeed, $CH_3O\cdot$ was experimentally trapped by PBN, yielding nitroxide **5** during photolysis of AZ-**3a**. The transition-state energy of the bond-breaking process in T-**DR3b** [$\Delta H^\ddagger$ = 75.7 kJ mol^{-1}, $\Delta G^\ddagger_{298}$ = 70.2 kJ mol^{-1} for exo-CH_3O and $\Delta H^\ddagger$ = 74.8 kJ mol^{-1}, $\Delta G^\ddagger_{298}$ = 67.8 kJ mol^{-1} for endo-CH_3O] was well consistent with the experimentally obtained activation values for the decay process of *π*-**3a** [E_a = 74.9 kJ mol^{-1}, $\Delta H^\ddagger$ = 72.1 kJ mol^{-1}, and $\Delta G^\ddagger_{298}$ = 73.4 kJ mol^{-1}].

To understand the nature of the *π*-single bonding in *π*-**3b**, the CASSCF calculation was conducted at the CASSCF(2,2)/6-31G(d) level of theory on *π*-**3b** optimized by density functional theory at the UB3LYP/6-31G(d) level of theory. As shown in Figure 3, the electron occupation numbers in the bonding orbital (*π*) and antibonding orbital (*π**) were 1.46 and 0.54, respectively. The bond order between the two radical carbons was 0.46. The diradical character (y_o)[34] was computed to be 0.24 and 0.37 at the CASSCF(2,2)/6-31G(d) and UB3LYP/6-31G(d) level of theory, respectively. As shown in Figure 3, the orbital coefficients were largely localized on the *π*-single bonding moiety because of metasubstitution in the macrocyclic moiety.

■ CONCLUSIONS

In conclusion, we developed a novel, relatively stable C−C *π*-single bonding system *π*-**3a** with singlet 1,3-diradical character. The *π*-single bonding species exhibits exceptional stability at room temperature, realized by switching the energy relationship between the *σ*- and *π*-bonds. Generally, the *σ*-bond is considerably more stable than the *π*-bond. However, the energy relationship between these bonds was reversed, owing to the molecular architecture derived from the macrocyclic ring. The newly developed *π*-bonding system has a significantly small HOMO−LUMO gap, leading to a new paradigm of molecular design for visible-to-NIR photoresponse and highly redox active compounds.

■ ASSOCIATED CONTENT

Supporting Information

The Supporting Information is available free of charge at https://pubs.acs.org/doi/10.1021/jacs.3c10971.

Movie S1 (MP4)

Materials and methods; general procedure for synthesizing the azoalkanes; synthesis of AZ-**3a**; structure assignment of AZ-**3a**; crystal data and structure refinement for AZ-**3a**; sub-microsecond transient absorption spectrum during the laser flash photolysis of AZ-**3a** at 293 K in benzene under vacuum condition; sub-microsecond transient absorption spectrum during the laser flash photolysis of AZ-**4a**/AZ-**4a** at 293 K in benzene under N_2; EPR spectra during the photolysis of AZ-**3a** (4.01 mM in a 2-methyltetrahydrofuran (MTHF) matrix at 88 K); transient absorption spectrum for the fall process of *π*-**3a** in toluene under vacuum condition; Arrhenius plots (left *y* axis, blue line) and Eyring plots (right *y* axis, redline) for the fall process of *π*-**3a** in toluene under vacuum condition from 243 K to 303 K; photochemical bleaching of *π*-**3a** in toluene under vacuum condition at 293 K; Eyring plots for the fall process of *π*-**3a** in toluene under argon atmosphere from 315 K to 360 K; Arrhenius plots (left *y* axis, blue line) and Eyring plots (right *y* axis, red line) for the rise process of *π*-**3a** in toluene under vacuum condition from 243 K to 303 K; AZ-**3a** denitrogenation after 10 min irradiation at room temperature in C_6D_6 under vacuum condition; high resolution mass spectrum (FD) of **4** spin-trapping experiments using electron paramagnetic response (EPR) measurements; energy profile of the reaction of *π*-**3b**; calculated intrinsic reaction coordinate paths for transition states; molecular strain energy (SE); calculated atomic coordinates (in Angstroms) and energies (in Hartrees) for all optimized structures (PDF)

Accession Codes

CCDC 2299337 contains the supplementary crystallographic data for this paper. These data can be obtained free of charge via www.ccdc.cam.ac.uk/data_request/cif, or by emailing data_request@ccdc.cam.ac.uk, or by contacting The Cambridge Crystallographic Data Centre, 12 Union Road, Cambridge CB2 1EZ, UK; fax: +44 1223 336033.

■ AUTHOR INFORMATION

Corresponding Author

Manabu Abe − *Department of Chemistry, Graduate School of Advanced Science and Engineering, Hiroshima University, Higashi-Hiroshima 739-8526 Hiroshima, Japan;* orcid.org/0000-0002-2013-4394; Email: mabe@hiroshima-u.ac.jp

Authors

Qian Liu − *Department of Chemistry, Graduate School of Advanced Science and Engineering, Hiroshima University, Higashi-Hiroshima 739-8526 Hiroshima, Japan*

Keita Onishi − *Department of Chemistry, Graduate School of Advanced Science and Engineering, Hiroshima University, Higashi-Hiroshima 739-8526 Hiroshima, Japan*

Yuki Miyazawa − *Department of Chemistry, Graduate School of Advanced Science and Engineering, Hiroshima University, Higashi-Hiroshima 739-8526 Hiroshima, Japan*

Zhe Wang − *Department of Chemistry, Graduate School of Advanced Science and Engineering, Hiroshima University, Higashi-Hiroshima 739-8526 Hiroshima, Japan;* orcid.org/0000-0002-9996-586X

Sayaka Hatano − *Department of Chemistry, Graduate School of Advanced Science and Engineering, Hiroshima University, Higashi-Hiroshima 739-8526 Hiroshima, Japan;* orcid.org/0000-0002-4745-2966

Complete contact information is available at: https://pubs.acs.org/10.1021/jacs.3c10971

Author Contributions

[†]Q.L. and K.O. authors contributed equally to this work.

Notes

The authors declare no competing financial interest.

■ ACKNOWLEDGMENTS

This work was supported by JSPS KAKENHI (grant nos. JP17H03022, 20K21197, 21H01921, and 22K19033) and JST CREST (JPMJCR18R4). We thank N-BARD, Hiroshima University, for the MS measurements. Q.L. would like to acknowledge the China Scholarship Council (CSC) for a Ph.D.

fellowship. This paper is dedicated to Professor Dennis Curran and Professor Shigeru Yamago on the occasion of their 70th and 60th birthday, respectively.

REFERENCES

(1) Luo, Y.-R. *Handbook of Bond Dissociation Energies in Organic Compounds*; CRC Press: Boca Raton, FL, 2002.

(2) Nicolaides, A.; Borden, W. T. Ab initio calculations of the relative strengths of the π bonds in acetylene and ethylene and of their effect on the relative energies of π-bond addition reactions. *J. Am. Chem. Soc.* **1991**, *113*, 6750−6755.

(3) Segura, J. L.; Martín, N.; Guldi, D. M. Materials for organic solar cells: the C_{60}/π-conjugated oligomer approach. *Chem. Soc. Rev.* **2005**, *34*, 31−47.

(4) Fitzner, R.; Mena-Osteritz, E.; Mishra, A.; Schulz, G.; Reinold, E.; Weil, M.; Körner, C.; Ziehlke, H.; Elschner, C.; Leo, K.; Riede, M.; Pfeiffer, M.; Uhrich, C.; Bäuerle, P. Correlation of π-Conjugated Oligomer Structure with Film Morphology and Organic Solar Cell Performance. *J. Am. Chem. Soc.* **2012**, *134*, 11064−11067.

(5) Liu, X.; Sun, Y.; Hsu, B. B. Y.; Lorbach, A.; Qi, L.; Heeger, A. J.; Bazan, G. C. Design and Properties of Intermediate-Sized Narrow Band-Gap Conjugated Molecules Relevant to Solution-Processed Organic Solar Cells. *J. Am. Chem. Soc.* **2014**, *136*, 5697−5708.

(6) Abe, M.; Adam, W.; Heidenfelder, T.; Nau, W. M.; Zhang, X. Intramolecular and intermolecular reactivity of localized singlet diradicals: The exceedingly long-lived 2,2-diethoxy-1,3-diphenylcyclopentane-1,3-diyl. *J. Am. Chem. Soc.* **2000**, *122*, 2019−2026.

(7) Adam, W.; Borden, W. T.; Burda, C.; Foster, H.; Heidenfelder, T.; Heubes, M.; Hrovat, D. A.; Kita, F.; Lewis, S. B.; Scheutzow, D.; Wirz, J. Transient spectroscopy of a derivative of 2,2-difluoro-1,3-diphenylcyclopentane-1,3-diyl-A persistent localized singlet 1,3-diradical. *J. Am. Chem. Soc.* **1998**, *120*, 593−594.

(8) Getty, S. J.; Hrovat, D. A.; Borden, W. T. Ab Initio Calculations on the Stereomutation of 1,1-Difluorocyclopropane. Prediction of a Substantial Preference for Coupled Disrotation of the Methylene Groups. *J. Am. Chem. Soc.* **1994**, *116*, 1521−1527.

(9) Abe, M.; Akisaka, R. Is π-single bonding (C-π-C) possible? A challenge in organic chemistry. *Chem. Lett.* **2017**, *46*, 1586−1592.

(10) Hoffmann, R.; Alder, R. W.; Wilcox, C. F. Planar Tetracoordinate Carbon. *J. Am. Chem. Soc.* **1970**, *92*, 4992−4993.

(11) Collins, J. B.; Dill, J. D.; Jemmis, E. D.; Apeloig, Y.; Schleyer, P. v. R.; Seeger, R.; Pople, J. A. Stabilization of Planar Tetracoordinate Carbon. *J. Am. Chem. Soc.* **1976**, *98*, 5419−5427.

(12) Priyakumar, U. D.; Sastry, G. N. A system with three contiguous planar tetracoordinate carbons is viable: A computational study on a $C_6H_6^{2+}$ isomer. *Tetrahedron Lett.* **2004**, *45*, 1515−1517.

(13) Abe, M.; Adam, W.; Hara, M.; Hattori, M.; Majima, T.; Nojima, M.; Tachibana, K.; Tojo, S. On the electronic character of localized singlet 2,2-dimethoxycyclopentane-1,3-diyl diradicals: Substituent effects on the lifetime. *J. Am. Chem. Soc.* **2002**, *124*, 6540−6541.

(14) Abe, M.; Tada, S.; Mizuno, T.; Yamasaki, K. Impact of Diradical Spin State (Singlet vs Triplet) and Structure (Puckered vs Planar) on the Photodenitrogenation Stereoselectivity of 2,3-Diazabicyclo[2.2.1]heptanes. *J. Phys. Chem. B* **2016**, *120*, 7217−7226.

(15) Ye, J.; Hatano, S.; Abe, M.; Kishi, R.; Murata, Y.; Nakano, M.; Adam, W. A Puckered Singlet Cyclopentane-1,3-diyl: Detection of the Third Isomer in Homolysis. *Chem.—Eur. J.* **2016**, *22*, 2299−2306.

(16) Scheschkewitz, D.; Amii, H.; Gornitzka, H.; Schoeller, W. W.; Bourissou, D.; Bertrand, G. Singlet diradicals: From transition states to crystalline compounds. *Science* **2002**, *295*, 1880−1881.

(17) Koike, T.; Osawa, R.; Ishida, S.; Iwamoto, T. Synthesis, Structure and Electronic Properties of a Stable π-Type 3-Electron-2-Center-Bonded Species: A Silicon Analogue of a Bicyclo[1.1.0]butane Radical Anion. *Angew. Chem., Int. Ed.* **2022**, *61*, No. e202117584.

(18) Majhi, P. K.; Zimmer, M.; Morgenstern, B.; Scheschkewitz, D. Transition-Metal Complexes of Heavier Cyclopropenes: Non-Dewar-Chatt-Duncanson Coordination and Facile Si=Ge Functionalization. *J. Am. Chem. Soc.* **2021**, *143*, 8981−8986.

(19) Yildiz, C. B.; Leszczyńska, K. I.; González-Gallardo, S.; Zimmer, M.; Azizoglu, A.; Biskup, T.; Kay, C. W. M.; Huch, V.; Rzepa, H. S.; Scheschkewitz, D. Equilibrium Formation of Stable All-Silicon Versions of 1,3-Cyclobutanediyl. *Angew. Chem., Int. Ed.* **2020**, *59*, 15087−15092.

(20) Kyushin, S.; Kurosaki, Y.; Otsuka, K.; Imai, H.; Ishida, S.; Kyomen, T.; Hanaya, M.; Matsumoto, H. Silicon-silicon π single bond. *Nat. Commun.* **2020**, *11*, 4009.

(21) Nukazawa, T.; Iwamoto, T. An Isolable Tetrasilicon Analogue of a Planar Bicyclo[1.1.0]butane with π-Type Single-Bonding Character. *J. Am. Chem. Soc.* **2020**, *142*, 9920−9924.

(22) Abe, M.; Furunaga, H.; Ma, D.; Gagliardi, L.; Bodwell, G. J. Stretch effects induced by molecular strain on weakening σ-bonds: Molecular design of long-lived diradicals (biradicals). *J. Org. Chem.* **2012**, *77*, 7612−7619.

(23) Diau, E. W.-G.; Abou-Zied, O. K.; Scala, A. A.; Zewail, A. H. Femtosecond dynamics of transition states and the concept of concertedness: Nitrogen extrusion of azomethane reactions. *J. Am. Chem. Soc.* **1998**, *120*, 3245−3246.

(24) Jelier, B. J.; Tripet, P. F.; Pietrasiak, E.; Franzoni, I.; Jeschke, G.; Togni, A. Radical Trifluoromethoxylation of Arenes Triggered by a Visible-Light-Mediated N-O Bond Redox Fragmentation. *Angew. Chem., Int. Ed.* **2018**, *57*, 13784−13789.

(25) Patrascu, B.; Mocanu, S.; Coman, A.; Madalan, A. M.; Popescu, C.; Paun, A.; Matache, M.; Ionita, P. Synthesis of fluorescent dansyl derivatives of methoxyamine and diphenylhydrazine as free radical precursors. *Int. J. Mol. Sci.* **2020**, *21*, 3559.

(26) Lee, C.; Yang, W.; Parr, R. G. Development of the Colle-Salvetti correlation-energy formula into a functional of the electron density. *Phys. Rev. B* **1988**, *37*, 785−789.

(27) Petersson, G. A.; Bennett, A.; Tensfeldt, T. G.; Al-Laham, M. A.; Shirley, W. A.; Mantzaris, J. A complete basis set model chemistry. I. The total energies of closed-shell atoms and hydrides of the first-row elements. *J. Chem. Phys.* **1988**, *89*, 2193−2218.

(28) Hegarty, D.; Robb, M. A. Application of unitary group methods to configuration interaction calculations. *Mol. Phys.* **1979**, *38*, 1795−1812.

(29) Miyazawa, Y.; Wang, Z.; Hatano, S.; Takagi, R.; Matsuoka, H.; Amamizu, N.; Kitagawa, Y.; Kayahara, E.; Yamago, S.; Abe, M. Generation and Characterization of a Tetraradical Embedded in a Curved Cyclic Paraphenylene Unit. *Chem.—Eur. J.* **2023**, *29*, No. e202301009.

(30) Wang, Z.; Akisaka, R.; Yabumoto, S.; Nakagawa, T.; Hatano, S.; Abe, M. Impact of the Macrocyclic Structure and Dynamic Solvent Effect on the Reactivity of a Localised Singlet Diradicaloid with π-Single Bonding Character. *Chem. Sci.* **2021**, *12*, 613−625.

(31) Wang, Z.; Yadav, P.; Abe, M. Long-Lived Localised Singlet Diradicaloids with Carbon-Carbon π-Single Bonding (C-π-C). *Chem. Commun.* **2021**, *57*, 11301−11309.

(32) Miyazawa, Y.; Wang, Z.; Matsumoto, M.; Hatano, S.; Antol, I.; Kayahara, E.; Yamago, S.; Abe, M. 1,3-Diradicals Embedded in Curved Paraphenylene Units: Singlet versus Triplet State and In-Plane Aromaticity. *J. Am. Chem. Soc.* **2021**, *143*, 7426−7439.

(33) Harada, Y.; Wang, Z.; Kumashiro, S.; Hatano, S.; Abe, M. Extremely Long Lived Localized Singlet Diradicals in a Macrocyclic Structure: A Case Study on the Stretch Effect. *Chem.—Eur. J.* **2018**, *24*, 14808−14815.

(34) Nakano, M.; Kishi, R.; Nitta, T.; Kubo, T.; Nakasuji, K.; Kamada, K.; Ohta, K.; Champagne, B.; Botek, E.; Yamaguchi, K. Second hyperpolarizability (γ) of singlet diradical system: Dependence of γ on the diradical character. *J. Phys. Chem. A* **2005**, *109*, 885−891.